Journal of the Korean Physical Society, Vol. 69, No. 7, October 2016, pp. 1187∼1190

Characteristics of the Oxygen Evolution Reaction on Synthetic Copper - Cobalt - Oxide Electrodes for Water Electrolysis

Yoo Sei Park, Chan Su Park, Chi Ho Kim and Yang Do Kim*
Department of Materials Science and Engineering, Pusan National University, Busan 46241, Korea

Sungkyun Park†
Department of Physics, Pusan National University, Busan 46241, Korea

Jae Ho Lee‡
Department of Materials Science and Engineering, Hongik University, Seoul 04066, Korea

(Received 16 August 2016, in final form 26 August 2016)

A nano-sized $Cu_{0.7}Co_{2.3}O_4$ powder was prepared using a thermal decomposition method to achieve an efficient anode catalyst for an economical water electrolysis system for high-purity hydrogen-gas production without using a noble-metal catalyst. This study showed that the calcination temperature should be maintained under 400 °C to obtain a spinel copper - cobalt oxide structure without secondary oxide phases. The powder calcined at 250 °C showed the highest current density at the oxygen evolution reaction. This was due mainly to the increased number of available active sites and the active surface area of the powders. Further systematic analyses of the electrochemical characteristics of $Cu_xCo_{3-x}O_4$ synthesized by using the fusion method were performed to assess it as potential anode material for use in alkaline-anion-exchange-membrane water electrolysis.

PACS numbers: 42.30.Rx, 42.40.Ht, 42.30.Kq
Keywords: Water electrolysis, Oxygen evolution reaction, $Cu_xCo_{3-x}O_4$ powders
DOI: 10.3938/jkps.69.1187

I. INTRODUCTION

Water electrolysis to H_2 and O_2 is an electrochemical method of hydrogen production, and water electrolyzers are promising devices for the production of hydrogen energy [1]. Three kinds of water electrolyzers are available: alkaline water electrolyzers (AWEs), polymer electrolyte membrane water electrolyzers (PEMWEs), and solid oxide steam electrolyzers (SOECs) [2]. Among them, PEMWEs show a high current density and can produce relatively high-purity hydrogen gas compared to other water electrolyzers [3, 4]. Recently, alkaline anion-exchange membrane (AAEM) water electrolysis has been proposed as an alternative approach and has attracted considerable interest [5]. Although the AAEM water electrolysis system can produce high-purity hydrogen without a noble-metal catalyst and does not require an additional drying step, issues regarding the anode overvoltage still exist [6,7].

*E-mail: yangdo@pusan.ac.kr; Fax: +82-51-510-0528
†E-mail: psk@pusan.ac.kr
‡E-mail: jhlee@hongik.ac.kr

In the water electrolysis reaction, the anode reaction, the oxygen-evolution reaction (OER), has problems with a large over-potential [8]. Noble metal oxides, such as RuO_2 and IrO_2, which have higher OER rates than other materials, are used as anode catalysts to overcome the large over-potential issue despite their high cost [9–11]. On the other hand, for commercial applications, low-cost, non-noble metals should be used for anode catalysts. Transition-metal oxides offer an alternative solution due to their low cost and excellent corrosion resistance, despite the low electrocatalytic activity for the OER [12–14]. In particular, spinel cobaltite oxides have been largely studied as anode catalysts for the OER. Furthermore, binary cobalt oxide is a good candidate because of its excellent electrical conductivity, availability, low cost, and high stability, as well as its being environmentally friendly [15]. Previously, $M_xCo_{3-x}O_4$ (M = Li, Ni, Cu), showed high electrocatalytic activity in the order of $Co_3O_4 < Ni_xCo_{3-x}O_4 << Cu_xCo_{3-x}O_4 < Li_xCo_{3-x}O_4$ [16]. Among these binary cobalt oxides, $Cu_xCo_{3-x}O_4$ is considered a promising anode catalyst because it is cost effective [17].

Various methods, such as the sol-gel technique, thermal decomposition, hydrothermal synthesis, and vacuum

sputtering, have been used to synthesize cost-effective anode catalysts [1,15,18–20]. The sol-gel method has advantages in producing highly porous surfaces with large active areas at relatively low temperatures. In addition, the precursor type significantly affects the properties of the catalysts [21–23]. Vacuum sputtering ensures precision and reproducibility and is unrelated to the type of metal precursor [24]. Thermal decomposition is normally used to fabricate fine metal-oxide powders. This method allows easy control of the particle size by controlling the calcination temperature [1,21]. In this study, $Cu_xCo_{3-x}O_4$ was synthesized by using a fusion method, and its electrochemical characteristics as a potential anode material for use in AAEM water electrolysis were analyzed systematically.

II. EXPERIMENTS

$Cu_xCo_{3-x}O_4$ powders were prepared by using the fusion method [25]. $CoCl_26H_2O$ and $CuCl_22H_2O$ were used as the starting materials. Both were dissolved simultaneously in 2-propanol with a total metal concentration of 0.2 mol/dm^3. The Cu/Co mole ratio was fixed to 0.7/2.3. The mixed solution was stirred for 3 hours at room temperature. Subsequently, a 50-fold excess of $NaNO_3$ was added to the solution and stirred for 48 hours. The solution was dried thoroughly at 70 °C and calcined at various temperatures (250 − 500 °C) for 1 hour in air. After heat treatment, the salt mixture was washed in deionized water to remove the residual salt and centrifuged to obtain nano-sized $Cu_xCo_{3-x}O_4$ powders.

The crystallinity and the crystal structure of the $Cu_{0.7}Co_{2.3}O_4$ powders were characterized by using X-ray diffraction (XRD). The morphology of the $Cu_xCo_{3-x}O_4$ was examined by using scanning electron microscopy (SEM). The particle size was analyzed by using a particle size analysis (PSA). The electrochemical properties of the catalysts were examined using a three-electrode cell in a 1-M KOH solution. Ag/AgCl (saturated KCl) was used as the reference electrode. The counter electrode was a Pt mesh.

The synthesized $Cu_{0.7}Co_{2.3}O_4$ powder and ionomer with a weight ratio of 98:2 were mixed in ethanol. After ultrasonication to produce dispersed powders, the ink was dropped onto a glassy carbon disk electrode with an area of 0.2 cm^2 and dried at 70 °C for 15 min in air. Before the electrochemical test, the KOH solution was bubbled with nitrogen gas for 30 min for the OER. The rotation speed of the disk electrode was kept constant at 2000 rpm for the OER study. The catalyst loading deposited on the glassy carbon electrode was approximately 0.34 mg/cm^2. Linear sweep voltammetry was conducted within a 200 ∼ 850 mV range (vs. Ag/AgCl saturated KCl) at a scan rate of 10 mV/s. Cyclic voltammetry was performed between 100 mV and 600 mV (vs. Ag/AgCl saturated KCl) at a scan rate of 50 mV/s.

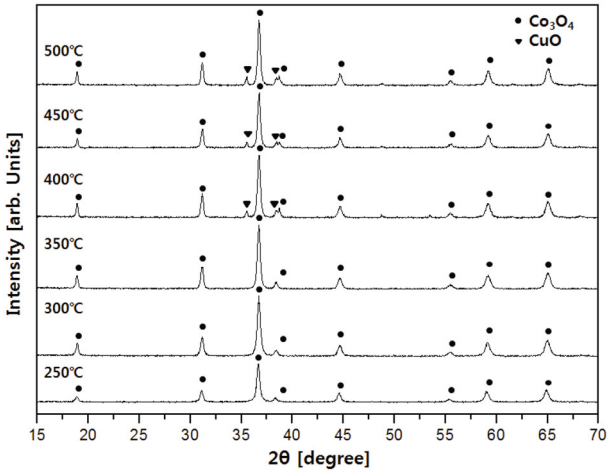

Fig. 1. XRD patterns of $Cu_{0.7}Co_{2.3}O_4$ powders calcined at temperatures in the range from 250 to 500 °C for 1 hour in air. The diffraction pattern of the powders calcined at 250 °C, 300 °C and 350 °C showed patterns identical to that of Co_3O_4. The powders calcined at higher temperatures exhibited additional CuO peaks.

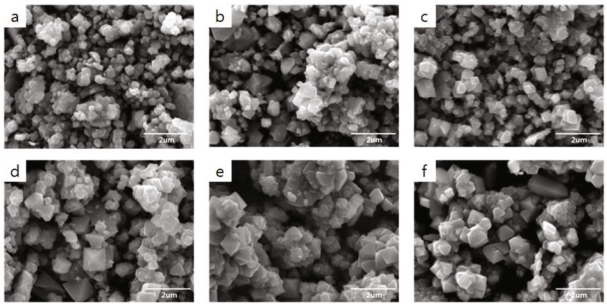

Fig. 2. SEM images of $Cu_{0.7}Co_{2.3}O_4$ powders calcined at (a) 250 °C, (b) 300 °C, (c) 350 °C, (d) 400 °C, (e) 450 °C and (f) 500 °C.

III. RESULTS AND DISCUSSION

Figure1 shows the XRD patterns of the $Cu_{0.7}Co_{2.3}O_4$ powders calcined at various temperatures (250 - 500 °C) for 1 hour in air. The samples calcined at temperatures between 250 °C and 350 °C exhibited XRD patterns identical to that of spinel Co_3O_4 (ICSD # 063164) while the samples calcined at temperatures above 400 °C showed additional CuO peaks at 35.53° and 38.44°. The formation of additional CuO peaks at calcination temperatures above 400 °C was similar to that previously reported [26]. This suggests that the calcination temperature should be maintained at a temperature under 400 °C to obtain a spinel copper-cobalt oxide structure without secondary oxide phases regardless of the synthesis method.

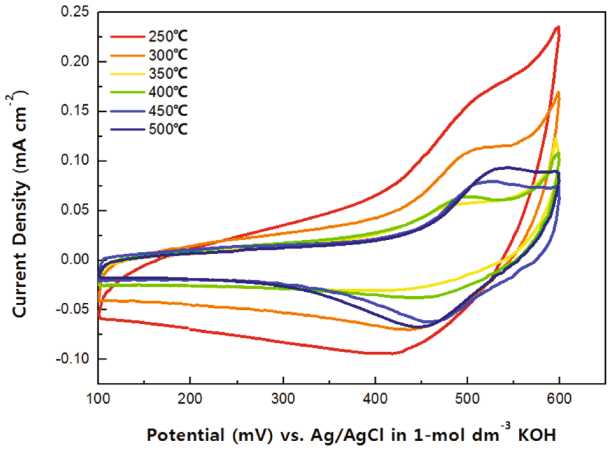

Fig. 3. (Color online) Cyclic voltammograms of $Cu_{0.7}Co_{2.3}O_4$ powders measured at 25 °C at a scan rate of 50 mV/s.

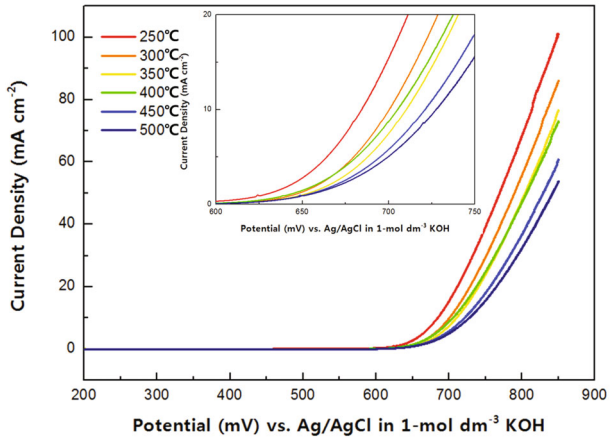

Fig. 4. (Color online) Linear sweep voltage of $Cu_{0.7}Co_{2.3}O_4$ powders calcined at various temperatures.

Figure 2 presents SEM images of $Cu_{0.7}Co_{2.3}O_4$ powders calcined at various temperatures. Agglomerated fine $Cu_{0.7}Co_{2.3}O_4$ powders with a relatively uniform size distribution were observed. On the other hand, an octagonal-shaped CuO phase with a large particle size started to appear at calcination temperatures above 400 °C. This result agreed with the XRD data. The mean particle size of the $Cu_{0.7}Co_{2.3}O_4$ powders generally increased with increasing calcination temperature. The mean particle size of the $Cu_{0.7}Co_{2.3}O_4$ powders calcined at various temperature was also analyzed by using a PSA. $Cu_{0.7}Co_{2.3}O_4$ powders calcined at 250 °C showed the smallest mean particle size of approximately 228 nm. The mean particle size increased from approximately 228 to 439 nm with increasing calcination temperature from 250 to 500 °C. The calculated crystallite size and unit cell dimensions were approximately 20 - 25 nm and 0.81 nm, respectively. The crystallite size and the unit cell dimension were calculated from the (311) planes.

Figure 3 presents the calcination temperature-dependent cyclic voltammograms. A relatively broad anodic peak was observed at approximately 490 ∼ 540 mV. The peak was assigned to the Co(IV)/Co(III) redox couple and appeared before the oxygen evolution reaction [2]. The peak potential generally shifted in a positive direction with increasing calcination temperature. The active area of the cyclic voltammogram for the $Cu_{0.7}Co_{2.3}O_4$ powders calcined at 250 °C was the largest compared to those of the powders calcined at relatively high temperatures. This suggests that calcination at a relatively low temperature is essential for synthesizing an active $Cu_{0.7}Co_{2.3}O_4$ catalyst.

Figure 4 shows the linear sweep voltammetry result for the OER. The potential required to obtain 10 mA cm^{-2} was the smallest in the sample calcined at 250 °C. The potentials were approximately 685 mV and 730 mV in the samples calcined at 250 °C and 500 °C, respectively. In addition, the $Cu_{0.7}Co_{2.3}O_4$ powder calcined at 250 °C showed the highest current density at the OER. The current density of the $Cu_{0.7}Co_{2.3}O_4$ powder calcined at 250 °C at 790 mV was approximately two times higher than that of the powder calcined at 500 °C. This is believed to be due mainly to the difference in the active areas. The smaller particle size of the $Cu_{0.7}Co_{2.3}O_4$ powders calcined at relatively low temperatures provided increases in the number of available active sites and in the active surface area.

IV. CONCLUSION

A nano-sized $Cu_{0.7}Co_{2.3}O_4$ powder was prepared using thermal decomposition methods at various calcination temperatures for anode catalyst applications in AAEM water electrolysis. The samples calcined at 250 - 350 °C exhibited XRD patterns identical to spinel Co_3O_4 while the samples calcined at temperatures above 400 °C showed the characteristic diffraction peaks of a Co_3O_4 and CuO mixture. Agglomerated fine $Cu_{0.7}Co_{2.3}O_4$ powders with a relatively uniform size distribution were observed. The mean particle size increased from approximately 228 to 439 nm with increasing calcination temperature from 250 to 500 °C. The active area of the cyclic voltammogram of $Cu_{0.7}Co_{2.3}O_4$ powders calcined at 250 °C was the largest compared to those calcined at relatively high temperatures. The $Cu_{0.7}Co_{2.3}O_4$ powder calcined at 250 °C showed the highest current density at the oxygen evolution reaction, which is believed to be due mainly to the increased number of available active sites and active surface area.

ACKNOWLEDGMENTS

This work was supported by the National Research Foundation of Korea (NRF) grant funded by the Ko-

rea government (MSIP) through GCRC-SOP (No. 2011-0030013) and the Human Resource Training Program for Regional Innovation and Creativity through the Ministry of Education and National Research Foundation of Korea (NRF-2014H1C1A1073088).

REFERENCES

[1] W. Xu, T. Jyoti, B. Suddhasatwa and S. Keith, Int. J. Hydrogen Energ. **36**, 14796 (2011).
[2] W. Xu and K. Scott, Int. J. Hydrogen Energ. **38**, 3123 (2013).
[3] M. Carmo, D. L. Fritz, J. Mergel and D. Stolten, Int. J. Hydrogen Energ. **38**, 4901 (2013).
[4] T. W. Koo, C. S. Park and Y. D. Kim, J. Korean Phys. Soc. **67**, 1558 (2015).
[5] X. Wu and K. Scott, J. Power Sources **206**, 14 (2012).
[6] A. V. Nikiforov, I. M. Petrushina, E. Christensen, N. V. Alexeev, A. V. Samokhin and N. J. Bjerrum, Int. J. Hydrogen Energ. **37**, 18597 (2012).
[7] G. Merle, M. Wessling and K. Nijmeijer, J. Memb. Sci. Rev. **377**, 1 (2011).
[8] F. Ferrara, Ph. D Thesis, University of Cagliari, Cagliari, France (2008).
[9] A. V. Nikiforov, I. M. Petrushina, E. Christensesn, N. V. Alexeev, A. V. Samokhin and N. J. Bjerrum, Int. J. Hydrogen Energ. **37**, 18591(2013).
[10] J. Cheng, H. Zhanga, G. Chena and Y. Zhang, Electrochim. Acta. **54**, 6250 (2009).
[11] M. E. G. Lyons and M. P. Brandon, Int. J. Electrochem. Sci. **3**, 1386 (2008).
[12] D. E. Hall, J. Electrochem. Soc. **130**, 317(1983).
[13] K. Kinoshita, *Electrochemical Oxygen Technology* (Wiley-Interscience, New York, 1992), p. 283.
[14] A. C. C. Tseung and S. Jasem, Electrochim. Acta. **22**, 31 (1977).
[15] M. Hamdani, R. N. Singh and P. Chartier, Int. J. Electrochem. Sci. **5**, 556 (2010).
[16] I. Nikolov, R. Darkaoui, E. Zhecheva, R. Stoyanova, N. Dimitrov and T. Vitanov, J. Electroanal. Chem. **429**, 157 (1997).
[17] M. De Koninck, S. C. Poirier and B. Marsan, J. Electrochem. Soc. **154**, A381 (2007).
[18] Y. Liu, C. Mi, L. Su and X. Zhang, Electrochimi. Acta. **53**, 2507 (2008).
[19] G. B. Barbi, J. P. Santos, P. Serrini, P. N. Gibson, M. C. Horrillo and L. Manes, Sensors Actuat B-Chem. **24/25**, 559 (1995).
[20] B. Lal, N. K. Singh, S. Samuel and R. N. Singh, J. New Mat. Electr. Sys. **2**, 59 (1999).
[21] A. Marshall, B. Boresen, G. Hagen, M. Tsypkin and R. Tunold, Mater. Chem. Phys. **94**, 226 (2005).
[22] M. De Koninck, S. C. Poirier and B. Marsan, J. Electrochem. Soc. **153**, 11A2103 (2006).
[23] T. A. F Lassali, J. F. C Boodts and L. O. S. Bulhões, J. Non-Cryst. Solids **273**, 129 (2000).
[24] Q. Zhang *et al*, Int. J. Hydrogen Energ. **37**, 822 (2012).
[25] V. Voorhees and R. Adams, J. Am. Chem. Soc. **44**, 1397 (1922).
[26] P. Paknahad, M. Askari and M. Ghorbanzadeh, Appl. Phys. A **119**, 727 (2015).